

Influence of the in-medium pion dispersion relation in heavy ion collisions

C. Fuchs, L. Sehn, E. Lehmann, J. Zipprich, and Amand Faessler

Institut für Theoretische Physik der Universität Tübingen, Auf der Morgenstelle 14, D-72076 Tübingen, Germany

(Received 6 September 1996)

We investigate the influence of medium corrections to the pion dispersion relation on the pion dynamics in intermediate energy heavy ion collisions. To do so a pion potential is extracted from the in-medium dispersion relation and used in QMD calculations and thus we take care of both, real and imaginary part of the pion optical potential. The potentials are determined from different sources, i.e., from the Δ -hole model and from phenomenological approaches. Depending on the strength of the potential, a reduction of the anticorrelation of pion and nucleon flow in noncentral collisions is observed as well as an enhancement of the high-energetic yield in transverse pion spectra. A comparison to experiments, in particular to p_t spectra for the reaction Ca+Ca at 1 GeV/nucleon and the pion in-plane flow in Ne+Pb collisions at 800 MeV/nucleon, generally favors a weak potential. [S0556-2813(97)03401-8]

PACS number(s): 25.75.-q, 13.75.Gx, 25.80.Ls

I. INTRODUCTION

The main motivation to study heavy-ion reactions at intermediate energies is to extract some information on nuclear matter under extreme conditions, i.e., at high densities and/or high temperatures. Besides nucleonic observables like the rapidity distribution and flow observables as, e.g., the bounce-off and squeeze-out, also mesons [π, K^+, η , etc.] emitted from the reaction zone can be probes of excited nuclear matter. Pion yields and spectra [3–8] turned out not to be sensitive to properties of the nucleon-nucleon interaction and difficult to interpret. Due to their strong interaction with the nuclear environment, pionic observables at the freeze-out are the result of complex creation and rescattering processes. However, pions can provide information about the resonance production in compressed and excited nuclear matter, in particular with respect to the $\Delta(1232)$ resonance which is the dominant production channel. In high-energetic collisions with heavy nuclei, the creation of “resonance matter,” i.e., a state with a density of Δ resonances comparable to the nuclear saturation density has, e.g., been discussed in this context [1,2].

Whereas total pion yields and low-energetic p_t spectra can be well explained by present theoretical transport approaches [9], the subthreshold production of high-energetic pions is a question of current debate. Such spectra have, e.g., been measured by the TAPS [5,6] and the KaoS [7] collaborations and at the Fragment Separator [8] at GSI. Various processes can contribute to the creation of subthreshold pions. One is the accumulation of energy by multistep collision processes, e.g., $\Delta\Delta$ scattering, but also heavier resonances as the $N^*(1440)$ can be excited and decay into high-energy pions. The analysis, in particular, of these high-energy p_t spectra is supposed to yield information about the role of resonances in heavy ion collisions [6]. However, both cases are rare and require a sufficiently high density of excited resonances, a state which mainly occurs in heavy systems. In lighter systems which have also been measured (Ar+Ca by TAPS [6] and Ni+Ni in Ref. [8]) multistep processes and the creation of higher resonances are less probable and it is not clear if these phenomena are sufficient to

explain the experimental data.

However, most theoretical approaches [9,10] included the interaction of the pions with the surrounding nuclear medium only by collision processes, i.e., parametrizing the imaginary part of the pion optical potential. In the present work we include also the real part of the pion optical potential which influences the pion propagation through the nuclear medium. We thus take care of the full in-medium pion optical potential. We investigate the influence on p_t spectra with pion momenta of several hundred MeV/c. This allows one to test the in-medium dispersion relation in the high-energy range.

To investigate the low-energy range of the dispersion relation, we consider the momenta of the pions in the collective in-plane pion flow which have values of some 10 MeV/c. The pion flow has been measured, e.g., by the DIOGENE group for the system Ne+Pb at 800 MeV/nucleon [11]. The prominent observation was there as an always positive pion flow in contrast to the typical S shape of the nucleon flow. This fact is probably due to the projectile-target geometry in this highly asymmetric system and the reabsorption of pions by the target matter, i.e., the so-called shadowing effect. In symmetric systems this shadowing effect may even lead to a complete anti-correlation of pion and nucleon flow [9,13]. Although conventional calculations, i.e., without a pion potential, are able to qualitatively reproduce the DIOGENE data [10,12], in particular, this (anti)correlation of flow reacts sensitively on the in-medium effects taken into account in the present work.

The knowledge of the pion optical potential from elastic pion-nucleus scattering is, however, restricted to nuclear densities at and below saturation and relatively small energies [14]. In intermediate energy heavy ion reactions up to 2 GeV incident energy per nucleon baryon densities of three times saturation density are reached and transverse momenta of about 1 GeV/c are detected in pion spectra. In this range the real part of the pion potential is almost unknown. Thus, one has to extrapolate the pion dispersion relation to the ranges relevant for heavy ion collisions. As done in Ref. [13], we apply two models, i.e., the Δ -hole model [15,16] and a phenomenological ansatz suggested by Gale and Kapusta [17]. The application of these models allows one to

investigate the influence of the possible boundary cases, i.e., a soft (Δ hole) and a rather strong phenomenological potential. Moreover, since the in-medium corrected dispersion relation suggested by Gale and Kapusta is close to the hypothetical pion condensation limit, it is a question of interest whether the boundary conditions occurring in intermediate energy heavy ion collisions would allow such a scenario. In addition, we apply a third potential which is a modification of the parametrization of Gale and Kapusta and lies in strength between the two former cases. In Ref. [13] we have demonstrated the influence on pionic flow observables in heavy ion collisions. Here we want to derive quantitative statements and to distinguish between the different approaches by comparison to experimental data, i.e., to p_t spectra of the emitted pions and the pion in-plane transverse flow produced in noncentral collisions.

The paper is organized as follows: First, we give an overview of the treatment of pions in the quantum molecular dynamics (QMD) approach, in particular, with respect to the resonances included and the collision processes. Next we discuss the dispersion relation and the resulting pion potentials, and then compare the results to experiment. Finally, a summary and an outlook is given.

II. PIONS IN QUANTUM MOLECULAR DYNAMICS

QMD is a semiclassical transport model which accounts for relevant quantum aspects like the Fermi motion of the nucleons, stochastic scattering processes including Pauli blocking in the final states, the creation and reabsorption of resonances, and the particle production. A detailed description of the QMD approach can be found in Refs. [18,19].

Each baryon is represented by a Gaussian wave packet with a fixed width L . The temporal evolution of the centroids of these wave packets is described by the classical equations of motion generated from an N -body Hamiltonian

$$\frac{\partial \mathbf{p}_i}{\partial t} = -\frac{\partial H_B}{\partial \mathbf{q}_i}, \quad \frac{\partial \mathbf{q}_i}{\partial t} = \frac{\partial H_B}{\partial \mathbf{p}_i} \quad (1)$$

with

$$H_B = \sum_i \sqrt{\mathbf{p}_i^2 + M_i^2} + \frac{1}{2} \sum_{\substack{i,j \\ (j \neq i)}} (U_{ij} + U_{ij}^{\text{Yuk}} + U_{ij}^{\text{Coul}}). \quad (2)$$

The Hamiltonian, Eq. (2), contains mutual two- (and three-) body potential interactions which are finally determined as classical expectation values from local Skyrme forces U_{ij} supplemented by a phenomenological momentum dependence and an effective Coulomb interaction U_{ij}^{Coul}

$$U_{ij} = \alpha \left(\frac{\rho_{ij}}{\rho_0} \right) + \beta \left(\frac{\rho_{ij}}{\rho_0} \right)^\gamma + \delta \ln^2(\epsilon |\mathbf{p}_i - \mathbf{p}_j|^2 + 1) \frac{\rho_{ij}}{\rho_0}, \quad (3)$$

$$U_{ij}^{\text{Coul}} = \left(\frac{Z}{A} \right)^2 \frac{e^2}{|\mathbf{q}_i - \mathbf{q}_j|} \text{erf} \left(\frac{|\mathbf{q}_i - \mathbf{q}_j|}{\sqrt{4L}} \right), \quad (4)$$

where ρ_{ij} is a two-body interaction density defined as

TABLE I. Inelastic scattering processes which are included in the present calculations.

$NN \leftrightarrow N\Delta$	$\Delta \leftrightarrow N\pi$
$NN \leftrightarrow NN^*$	$N^* \leftrightarrow N\pi$
$NN \rightarrow \Delta\Delta$	$N^* \rightarrow \Delta\pi$
$N\Delta \rightarrow \Delta\Delta$	$N^* \rightarrow N\pi\pi$

$$\rho_{ij} = \frac{1}{(4\pi L)^{3/2}} e^{-(\mathbf{q}_i - \mathbf{q}_j)^2/4L} \quad (5)$$

and erf is the error function. The parameters $\alpha, \beta, \gamma, \delta, \epsilon$ of the Skyrme interaction, Eq. (3), are determined in order to reproduce simultaneously, the saturation density ($\rho_0 = 0.16 \text{ fm}^{-3}$) and the binding energy ($E_B = -16 \text{ MeV}$) for normal nuclear matter for a given incompressibility as well as the correct momentum dependence of the real part of the nucleon-nucleus optical potential [19,20]. In the present calculations we apply the standard parametrization of a hard/soft equation of state ($K = 380/200 \text{ MeV}$). The Yukawa-type potential U_{ij}^{Yuk} in Eq. (2) mainly serves to improve the surface properties and the stability of the initialized nuclei.

Analogously to the baryons, Eq. (2), the mesons also obey Hamilton's equations of motion. The Hamiltonian of the pions, i.e., the sum of the respective single particle energies ω_i , is represented in a mean field form

$$H_\pi = \sum_i^{N_\pi} \omega_i = \sum_i^{N_\pi} [\sqrt{\mathbf{p}_i^2 + m_\pi^2} + \text{Re}V_\pi^{\text{opt}}(\mathbf{p}_i, \mathbf{q}_i)], \quad (6)$$

where N_π is the actual number of pions. The dependence of the pionic mean field, i.e., the real part of the pion optical potential $\text{Re}V_\pi^{\text{opt}}$, on the pion coordinates originates from the medium effects in dense nuclear matter. Such medium effects are naturally expressed through a density dependence and $\text{Re}V_\pi^{\text{opt}}$ takes the form

$$\text{Re}V_\pi^{\text{opt}}(\mathbf{p}_i, \mathbf{q}_i) = \text{Re}V_\pi^{\text{opt}}[\mathbf{p}_i, \rho_B(\mathbf{q}_i)], \quad (7)$$

where ρ_B is the respective baryon density. In conventional approaches [9,10] the Hamiltonian, Eq. (7), is taken as that of the vacuum, i.e., $\text{Re}V_\pi^{\text{opt}}$ is set equal zero.

Hard core scattering of the particles is included by the simulation of the collision processes by standard Monte Carlo procedures. The collisions' probabilities are determined by a geometrical minimal distance criterion $d \leq \sqrt{\sigma_{\text{tot}}}/\pi$ weighted by the Pauli blocking factors of the final states [18,21]. For the inelastic nucleon-nucleon channels we include the $\Delta(1232)$ as well as the $N^*(1440)$ resonance. In the intermediate energy range, the resonance production is dominated by the Δ ; however, the N^* yet gives non-negligible contributions to the high-energetic pion yield [1]. The resonances as well as the pions originating from their decay are explicitly treated, i.e., in a nonperturbative way and all relevant channels are taken into account. In particular, we include the resonance production and rescattering by inelastic NN collisions, the one-pion decay of Δ and N^* , and the two-pion decay of the N^* and one-pion reabsorption processes. These are summarized in Table I where

the isospin dependence of the various channels is suppressed for the sake of simplicity; which is, however, taken into account in the calculations.

For the cross sections of the inelastic NN channels, we adopt the parametrizations of Ref. [22] which have been determined from one-boson-exchange amplitudes in a Born approximation. The lifetimes of the resonances are determined through their energy and momentum dependent decay widths

$$\Gamma(|\mathbf{p}|) = \frac{a_1 |\mathbf{p}|^3}{(1 + a_2 |\mathbf{p}|^2)(a_3 + |\mathbf{p}|^2)} \Gamma_0, \quad (8)$$

which originates from the p -wave representation of the resonances. In Eq. (8) \mathbf{p} is the momentum of the created pion (in GeV/ c) in the resonance rest frame. According to Ref. [22] the values $a_1 = 22.83$ (28.8), $a_2 = 39.7$, and $a_3 = 0.04$ (0.09) are used for the Δ (N^*), and the bare decay widths are taken as $\Gamma_0^\Delta = 120$ MeV and $\Gamma_0^{N^*} = 200$ MeV. The reabsorption cross sections ($\pi N \rightarrow \Delta, N^*$) are determined assuming a Breit-Wigner distribution for the masses, i.e.,

$$\sigma = \frac{\sigma_0}{\mathbf{p}^2 (M_R \Gamma_R)^2} \frac{1}{(s - M_R^2)^2 + (M_R \Gamma_R)^2}, \quad (9)$$

where R stands for a Δ or N^* and \mathbf{p} is the c.m. momentum. In contrast to, e.g., Ref. [10] the momentum dependent resonance width, Eq. (8) is used in Eq. (9). The resonance rescattering cross section [$N(\Delta, N^*) \rightarrow NN$] is determined from a detailed balance. To take care of the proper phase space available for this channel, we take the finite width of the resonances into account as proposed in Ref. [23]. In particular for pions near the Δ threshold this procedure leads to a significant enhancement of the rescattering cross section and the low-energetic pion yield is suppressed by about 30%. Thus, we are able to reasonably reproduce the total pion multiplicities with results similar to Ref. [9].

In the presence of a pion potential, this has to be taken into account in the energy balance in order to ensure energy conservation in the collision processes, i.e., the relation

$$\sqrt{\mathbf{p}_R^2 + M_R^2} = \sqrt{(\mathbf{p}_R - \mathbf{p}_\pi)^2 + M_N^2} + \sqrt{\mathbf{p}_\pi^2 + m_\pi^2} + \text{Re}V_\pi^{\text{opt}}(\mathbf{p}_\pi, \rho_B) \quad (10)$$

has to be fulfilled. Concerning the pion reabsorption, Eq. (10) is exactly fulfilled; in the case of a resonance decay, this procedure is more involved since the decay takes place in the resonance rest frame. The potential of the created pion depends, however, on its momentum in the rest frame of the colliding nuclei. Thus, the pion momentum is determined iteratively until Eq. (10) is fulfilled with an accuracy better than 0.5 MeV which corresponds to an energy violation of less than about 0.04%.

Although the elementary cross sections [22] are parametrizations of the free cross sections, medium corrections to the imaginary part of the pion optical potential are included firstly by the enhancement of the rescattering/reabsorption probability which is proportional to the nuclear density, i.e., the available scattering partners, and secondly by the Pauli blocking in the final states according to the respective phase space occupancy. Via Eq. (10) also the real part of the pion potential gives corrections to the imaginary part. Thus, the

mean free path of the pions is significantly reduced and a consistent treatment of the real and imaginary part of the optical potential is achieved. Furthermore, the momentum dependence of the nuclear mean field, Eq. (3), results in a (nonrelativistic) effective mass of the baryons.

III. THE PION POTENTIAL

In contrast to the imaginary part of the pion optical potential which is well known from inelastic pion-nucleus scattering, the knowledge of the real part extracted from elastic pion-nucleus scattering is rare and restricted to low energies [14]. Data are available only for momenta up to about $2 m_\pi c$. However, in intermediate energy heavy ion reactions, pion momenta of more than 1 GeV/ c can occur and the high-energy tails of the pion spectra are of particular interest since they are supposed to yield information about the resonance production in hot and dense nuclear matter and corresponding in-medium effects [5,6,8]. Furthermore, nuclear densities up to three times saturation density can be reached whereas the elastic pion-nucleus scattering is restricted to densities around saturation and below. Thus, one has to extrapolate the dispersion relation to the energy range relevant for heavy ion collisions. However, such an extrapolation is affected by large uncertainties. To cover the unknown ranges, we apply two contrary approaches, i.e., a microscopic and a phenomenological ansatz for the pion dispersion relation.

The microscopic ansatz is based on the perturbation expansion of the Δ -hole model [15]. The summation of the Δ -hole polarization graphs results in a pion self-energy Π entering into the in-medium pion dispersion relation

$$\omega(\mathbf{p})^2 = \mathbf{p}^2 + m_\pi^2 + \Pi(\omega, \mathbf{p}, \rho_B). \quad (11)$$

Here the self-energy depends on the energy ω and the momentum \mathbf{p} of the pion and on the nuclear matter density ρ_B . In the framework of the Δ -hole model, the self-energy is finally given in the form

$$\Pi(\omega, \mathbf{p}, \rho_B) = \frac{\mathbf{p}^2 \chi(\omega, \mathbf{p}, \rho_B)}{1 - g' \chi(\omega, \mathbf{p}, \rho_B)} \quad (12)$$

with

$$\chi(\omega, \mathbf{p}, \rho_B) = -\frac{8}{9} \left(\frac{f_\Delta}{m_\pi} \right)^2 \frac{\omega_\Delta(\mathbf{p}) \rho_B}{\omega_\Delta^2(\mathbf{p}) - \omega^2(\mathbf{p})},$$

$$\omega_\Delta = \sqrt{M_\Delta^2 + \mathbf{p}^2} - M_N.$$

The parameters entering into Eq. (12), in particular, the $\pi N \Delta$ coupling constant f_Δ and the correlation parameter g' are taken in consistence with the OBE parameters of Ref. [22] and a consistent treatment of the real and imaginary part of the pion optical potential is achieved.

Although this approach works reasonably well at low baryon densities and low pion momenta [16], one has to be careful when applying Eq. (12) to heavy ion reactions. The self-energy obtained from the Δ -hole model includes, in addition to the excitation of ΔN^{-1} states, also short-range correlations of these states. In this approximation one neglects, however, terms of higher order [24] which are necessary to prevent the system from undergoing a phase transition to the

so-called pion condensation. Furthermore, Eq. (11) yields the wrong boundary conditions for high-energy pions when they pass through the surface of nuclear matter into the vacuum, in particular, a “quasi-pion” expressed by a Δ -hole state has to convert asymptotically to a real pion which can be detected. A common practice to avoid these unphysical features is to mix the two solutions of the dispersion relation, Eq. (11), i.e., the pionlike and the Δ -hole-like branch (Ω_1, Ω_2) in order to obtain an effective pion dispersion relation [25]

$$\omega_{\text{eff}} = Z_1 \Omega_1 + Z_2 \Omega_2, \quad Z_1 + Z_2 = 1. \quad (13)$$

The probabilities for the quasipion to sit on the pionlike branch (Z_1) or the Δ -hole-like branch (Z_2) are determined from the condition

$$\frac{1}{\omega^2 - \mathbf{p}^2 - m_\pi^2 - \Pi} = \frac{Z_1}{\omega^2 - \Omega_1^2} + \frac{Z_2}{\omega^2 - \Omega_2^2} \quad (14)$$

and thus the physical boundary conditions are fulfilled. Replacing ω in Eq. (11) by ω_{eff} , one obtains an effective pion self-energy Π_{eff} . The real part of the optical potential is obtained from the pion wave equation, i.e., the Klein-Gordon equation as [15]

$$\text{Re}V_\pi^{\text{opt}}(\mathbf{p}, \rho_B) = \frac{\Pi_{\text{eff}}(\omega_{\text{eff}}, \mathbf{p}, \rho_B)}{2\omega_{\text{eff}}}. \quad (15)$$

The density and momentum dependence of the dispersion relation are shown in Fig. 1 and it is seen that such a construction leads to a strong softening of the in-medium effects compared, e.g., to the original dispersion relation [25]. Consequently, the medium dependence of the resulting potential, Eq. (15), (called Pot. 1 in the following and shown in Fig. 1) is moderate and the attraction of the potential is weak. Hence, one cannot be sure that the modified dispersion relation still represents the true pion-nucleon interaction.

As already done in Ref. [13], we also consider a phenomenological ansatz suggested by Gale and Kapusta [17]. The dispersion relation then reads

$$\omega(p) = \sqrt{(|\mathbf{p}| - p_0)^2 + m_0^2} - U, \quad (16)$$

$$U = \sqrt{p_0^2 + m_0^2} - m_\pi, \quad (17)$$

$$m_0 = m_\pi + 6.5(1 - x^{10})m_\pi, \quad (18)$$

$$p_0^2 = (1 - x)^2 m_\pi^2 + 2m_0 m_\pi (1 - x). \quad (19)$$

A phenomenological medium dependence is introduced via $x = e^{-a(\rho_B/\rho_0)}$ with the parameter $a = 0.154$ and ρ_0 the saturation density in nuclear matter (here $\rho_0 = 0.16 \text{ fm}^{-3}$). The form of Eqs. (16)–(18) is motivated by the following constraints [17]:

- (i) The group velocity $\partial\omega/\partial p$ may not exceed the velocity of light.
- (ii) For high-energetic pions many-body effects should be of minor importance and ω should in leading order be proportional to p for $p \rightarrow \infty$.
- (iii) Corresponding to a strong p -wave interaction, the energy should have a minimum.

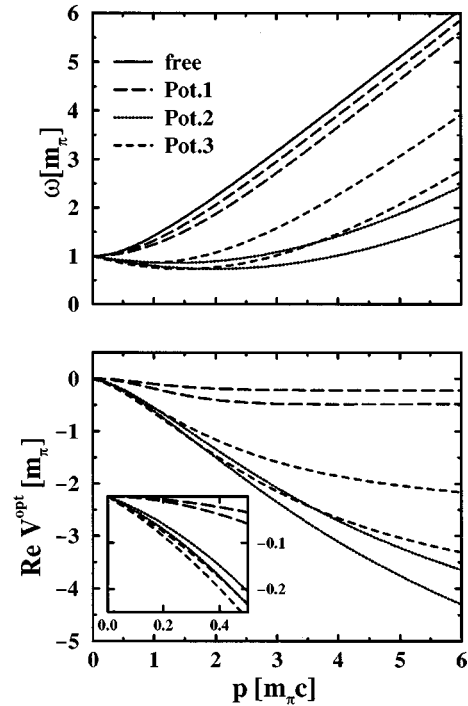


FIG. 1. Upper figure: The free pion dispersion relation (solid) is compared to various in-medium dispersion relations at nuclear densities $\rho_B = \rho_0$ (respective upper curves) and $\rho_B = 2\rho_0$ (respective lower curves). The in-medium dispersion relation is extracted from the Δ -hole model (Pot. 1, long dashed) and the phenomenological parametrization of Ref. [17] (Pot. 2, dotted) as well as a softer parametrization (Pot. 3, dashed) are shown. Lower figure: Real part of the pion optical potential at densities $\rho_B = \rho_0$ (upper curves) and $\rho_B = 2\rho_0$ (lower curves) extracted from the corresponding dispersion relations. The inserted figure zooms the low momentum range.

- (iv) Due to a weak s -wave interaction, medium effects are weak for pions at rest with respect to the surrounding medium.
- (v) The observation of pionic atoms implies that $\omega \approx -20 \text{ MeV}$ for $\rho_B = \rho_0$ and $p \approx 2m_\pi c$.
- (vi) Pion condensation can only appear at infinite density.

The dispersion relation as well as the corresponding potential (called Pot. 2 in the following) are shown in Fig. 1. Here $\text{Re}V_\pi^{\text{opt}}$ is extracted from Eq. (16) as $\text{Re}V_\pi^{\text{opt}} = \omega - \sqrt{\mathbf{p}^2 + m_\pi^2}$. It turns out that the potential is much stronger and its medium dependence is much more pronounced than in the case of the modified Δ -hole dispersion relation. In this context we want to mention that this effect is to a large extent due to the mixing of the pionlike and the Δ -hole-like branches in Pot. 1 since a potential extracted according Eq. (16) from the pure pionlike branch given in the Δ -hole model is of the same magnitude as Pot. 2 [26]. Thus, Pot. 1 and Pot. 2 can be looked as the boundary cases of a rather weak and a very strong pion potential. Furthermore, the phenomenological dispersion relation 2 is closer to the limit where pion condensation can occur.

In order to test the pion dispersion relation, it is, therefore, a natural step to suggest a third parametrization (Pot. 3)

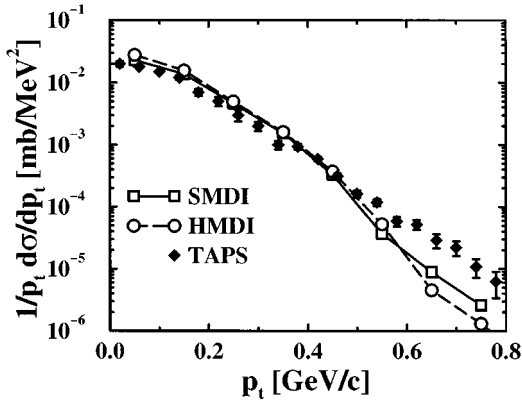


FIG. 2. Influence of the nuclear EOS on the π^0 p_t spectrum for the reaction $^{40}\text{Ca}+^{40}\text{Ca}$ at 1 GeV/nucleon. Hard (HMDI) and soft (SMDI) momentum dependent Skyrme forces have been used. The experimental data have been measured by the TAPS Collaboration for the system $^{40}\text{Ar}+^{40}\text{Ca}$ at 1 GeV/nucleon [6].

which lies in between the former ones. To do so, we decrease the power x^{10} in Eq. (18) to x^2 . The constraints (i)–(iv) remain unrendered by this modification except of point (v) where now a value of +10 MeV is obtained instead of -15 MeV in the former case. However, we do not consider this as a severe drawback since the application of the potential to heavy ion collisions should not be affected therefrom. In addition, also the Δ -hole model potential does not yield a bound quasihion for these values of ρ_B and p .

IV. RESULTS

First we consider transverse momentum p_t spectra for the system $^{40}\text{Ca}+^{40}\text{Ca}$ at 1 GeV incident energy per nucleon. In particular, we compare the π^0 spectra recently measured by the TAPS collaboration [6]. Here the π^0 's have the advantage that they are not distorted by Coulomb effects. The calculations are impact parameter averaged and a rapidity cut of $-0.2 \leq y_{\text{c.m.}} \leq 0.2$ has been applied which takes into account the detector acceptance. The data shown in Figs. 2 and 3 have been obtained with this cut [27] and are slightly enhanced with respect to the results shown in Ref. [6] where a larger cut has been used. In Fig. 2 we first investigate the influence of the nuclear equation of state and, therefore, compare a soft (SMDI) and a hard (HMDI) momentum dependent Skyrme force, see Eq. (3). It is seen that the dependence of the pion spectrum on the nuclear EOS is moderate and the agreement with the data is reasonable, however, not overwhelmingly good. We want to mention that the results obtained with the hard EOS are close to those of Ref. [9]. As also found there the low p_t spectrum is slightly overestimated whereas the high p_t range is underestimated by about a factor of 3. In Ref. [9] the lack of high energy pions is even more pronounced than in the present calculations. This is probably due to the $N^*(1440)$ resonance which was not taken into account there.

Next we turn to the influence of the in-medium pion potential. In Fig. 3 we show the π^0 -spectra for the same reaction as in Fig. 2 now include the pion-nucleon interaction as discussed in the previous section. All calculations are performed with the soft momentum dependent Skyrme force. It

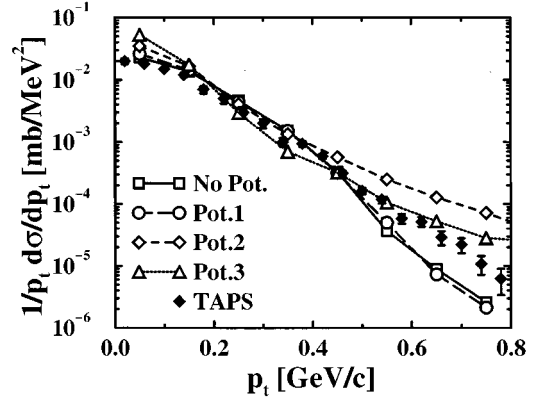


FIG. 3. Influence of the in-medium pion potential on the π^0 p_t spectrum for the same reaction as in Fig. 2. The calculations are performed without (solid) and include a pion potential. The respective potentials have been obtained from the Δ -hole model (Pot. 1) and by the phenomenological ansatz of Ref. [17] (Pot. 2). Pot. 3 corresponds to a modification of Pot. 2.

is seen that the weak Δ -hole potential (Pot. 1) has nearly no influence on the p_t spectrum which is in agreement with the results of Ref. [25] where a similar potential has been investigated. In this context we want to mention that concerning the low-energy pions, the present results (and those of Ref. [9]) stand somehow in contradiction to the BUU calculations of Refs. [25,26] since the significantly underestimated low-energy p_t yields were obtained when the pion potential was neglected. However, in these works comparisons to other measurements have been performed [28,29]. In our opinion the discrepancies are rather caused by the analysis of the data than by a slightly different treatment of the pion creation and annihilation processes outlined in Sec. II.

In the case of the phenomenological potentials 2 and 3, the situation is completely different now. With Pot. 2 the low p_t range is slightly enhanced, however, the high-energy pions are overestimated by nearly one order of magnitude. Such an enhancement of low-energy pions has been observed in Ref. [26] where an effective pion potential has also been determined within the Δ -hole model which is, however, apparently stronger than Pot. 1 in the present work. This complex behavior can be understood by the strong attraction of the respective potential which forces the pions to follow the trajectories of the nucleons. Most pions get bound by the stopped participant matter resulting in an enhancement of the low p_t yield. On the other hand, pions which are bound by the spectator matter are driven out to high transverse momenta by the nucleonic flow and thus the high p_t range is strongly enhanced. This effect is diminished when the potential is weaker (Pot. 3). Here the very high-energy yield ($p_t \geq 0.7$ GeV/c) is still slightly overestimated but also the low p_t range is now overestimated by about a factor of 3. The latter is understandable since for low momenta ($p \leq 1.5m_\pi c$) Pot. 3 is even stronger than Pot. 2, see zoomed region in Fig. 1.

The above observations are clearly reflected in the pion transverse flow. In Fig. 4 we compare the pion and the baryon in-plane transverse flow for the reaction $\text{Ca}+\text{Ca}$ at 1 GeV/nucleon. The results are impact parameter averaged and scaled to the pion and nucleon mass, respectively. By this

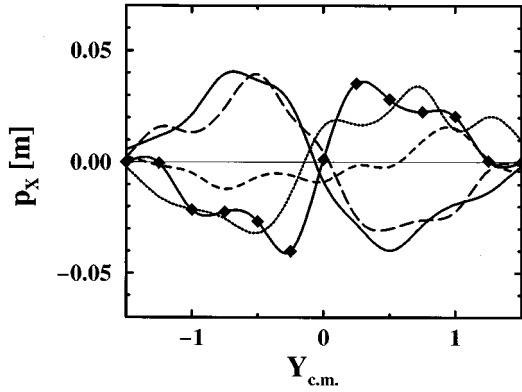


FIG. 4. Influence of the in-medium pion potential on the in-plane transverse pion flow as a function of the center-of-mass rapidity for the same reaction as in Fig. 2. The calculations are performed without (solid) and with inclusion of a pion potential. The respective potentials have been obtained from the Δ -hole model (Pot. 1, long dashed) and by the phenomenological ansatz of Ref. [17] (Pot. 2, dotted). Pot. 3 (dashed) corresponds to a modification of Pot. 2. In addition, the nucleon flow is shown (solid with diamonds). The results are scaled to the pion and nucleon mass and thus the transverse flow is given in units of $m_\pi c$ and $m_N c$, respectively.

scaling pion and nucleon flow are of the same order of magnitude. It is seen that without any pion-nucleon interaction, the flow of pions and nucleons is clearly anticorrelated. The anticorrelation originates from the absorption of the pions by the participant matter which produces the nucleonic flow. This is known as the shadowing effect. In the presence of the weak Δ -hole potential (Pot. 1) the pion flow remains nearly the same. In the case of Pot. 2 the pion flow switches from an anticorrelation to a correlation with the nucleon flow, i.e., the pions are forced to follow the trajectories of the spectator nucleons by the strong attractive potential. Further, it is seen that the strength of Pot. 3 has just a magnitude where the attraction and the shadowing effect are nearly completely counterbalanced and the resulting flow is around zero. This overall behavior is in good agreement with the interpretation of p_t spectra given above.

In summary none of the cases under consideration is able to reproduce the experimental spectrum over the entire range of energy with a satisfying high accuracy. Both, the low as well as the high p_t range react sensitively on the pion potential. Pot. 2 seems to be too attractive and can be ruled out by the comparison to the data. However, the present results indicate that the inclusion of higher resonances may not be sufficient to explain the role of high-energy pions, but further going medium effects should be taken into account.

Next we investigate the collective in-plane transverse flow of pions which has been measured for the system Ne+Pb at 800 MeV/nucleon by the DIOGENE Collaboration [11]. There the most striking results were the observation of a positive pion flow also for backwards rapidities, i.e., the pion flow is partially anticorrelated to the nucleon flow. In particular, here we consider a semicentral reaction at impact parameter $b=3$ fm. For a comparison with the data, we included the experimental detector filter cuts given in Ref. [11]. In addition, we simulated the reconstruction of the estimated reaction plane as it was done in the experimental

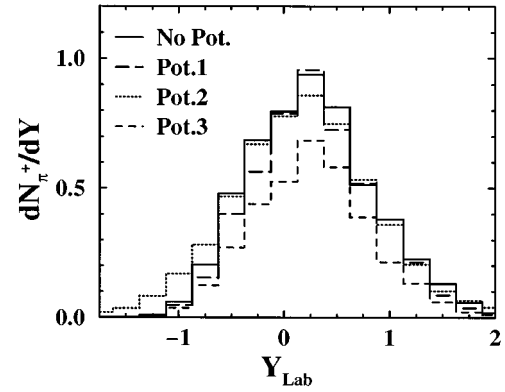


FIG. 5. π^+ rapidity distribution for a semicentral ($b=3$ fm) Ne on Pb reaction at 800 MeV/nucleon after applying the experimental detector filter cut. The calculations are performed without (solid) and include a pion potential. The respective potentials have been obtained from the Δ -hole model (Pot. 1, long dashed) and by the phenomenological ansatz of Ref. [17] (Pot. 2, dotted). Pot. 3 corresponds to a modification of Pot. 2.

analysis. In contrast to the theoretical calculation where the true reaction plane is known *a priori* in the experiment, the transverse in-plane vector is estimated for every event by

$$\mathbf{Q} = \sum_j \omega_j \mathbf{p}_{\perp j}, \quad (20)$$

where the sum runs over all detected protons weighted by their relative rapidity $\omega_j = y_i - \langle y \rangle$ with $\langle y \rangle$ the mean rapidity of the total system. The estimated in-plan pion momentum $p_x = \mathbf{p}_{\perp} \cdot \hat{\mathbf{Q}}$ is then obtained by the projection on the unit vector $\hat{\mathbf{Q}}$.

Figure 5 shows the corresponding π^+ rapidity distribution obtained with the various pion potentials and including the detector cuts. The calculation without pion potential is thereby in a good agreement with the result of Ref. [10]. The influence of the pion potentials 1 and 2 on the longitudinal flow is relatively weak, only in the case of Pot. 2 a slight enhancement of the backward, i.e., the targetlike, rapidity distribution is observed. Applying Pot. 3 we observe a strong suppression of the detected π^+ yield over the entire rapidity range. This effect is also reflected in the total yields given in Table II; is, however, not so pronounced since the total yield is only suppressed by about 10%. In general the usage of a potential leads to a slight reduction of the total yields which was also found in Refs. [25,26]. Concerning Pot. 3 the effect seen in Fig. 5 seems to be somehow an artifact of the detector geometry. Nevertheless, the dynamics of the pions is significantly changed and slow pions near the Δ threshold get,

TABLE II. Total π^+ yield (without experimental filter) and the ratio R of detected π^+ and π^- pions with positive to negative values of p_x for the reaction Ne on Pb at 800 MeV/nucleon and impact parameter $b=3$ fm. The experimental value for R is an average of the respective values for π^- and π^+ given in Ref. [11].

	No Pot.	Pot. 1	Pot. 2	Pot. 3	Exp.
N_{π^+}	1.89	1.86	1.80	1.59	
R	1.26	1.25	1.03	1.12	1.34

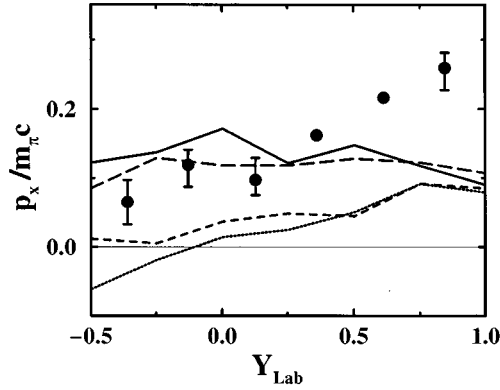


FIG. 6. Transverse in-plane flow per pion scaled to the pion mass for a semicentral ($b=3$ fm) Ne on Pb reaction at 800 MeV/nucleon after applying the experimental detector filter cut. The calculations are performed without (solid) and include a pion potential. The same potentials as in Fig. 5 have been used, i.e., Pot. 1 (long dashed), Pot. 2 (dotted), and Pot. 3 (dashed). The data are taken from Ref. [11].

in particular, strongly bound and are preferentially reabsorbed by the spectator matter.

In Fig. 6 the corresponding in-plane flow per pion is shown in units of the pion mass. Here the procedure to reconstruct the experimental reaction plane has been performed. It turns out that in the case of a vanishing or a weak potential (Pot. 1), the flow is always positive and in a fairly good agreement with the data for values around midrapidity. In the high forward rapidity range we, however, underestimate the data by about a factor of 2. Since the results are strongly distorted by the large asymmetry of the considered system and the reconstruction of the reaction plane, this effect can be due to a lack of sufficiently good statistics in this range. The positive flow at backward rapidities is explained by the reabsorption of the pions by the large target and thus is a consequence of the shadowing effect. In the case of the strong Pot. 2, the shadowing effect is overcompensated by the attraction of the potential and the flow shows a definite change of sign from negative to positive values at midrapidity. Similarly as in Fig. 4 Pot. 3 shows the same behavior which is, however, not so pronounced. Both, Pot. 2 and 3 yield significantly too less positive flow over the entire rapidity range.

These observations are also reflected in the ratio R between the numbers of pions with positive and negative values of p_x displayed in Table. II. Since we did not explicitly include the Coulomb interaction in the propagation of the pions, Eqs. (1) and (6), the different charge states are only taken into account via the isospin dependence of the respective creation/absorption channels. Thus, for a fair comparison to the measured ratio a mean value (corrected for the respective total yields) of π^+ ($R=1.42$) and π^- ($R=1.30$) which is about $R=1.34$ should be compared. Then the theoretical positive p_x abundancy is in reasonable agreement with the experiment for the calculations without potential and with Pot. 1. In the case of Pot. 2 and Pot. 3, however, R is close to unity.

V. SUMMARY AND CONCLUSIONS

We investigated the influence of medium corrections to the pion dispersion relation on the pion dynamics in heavy ion collisions. This was done by the introduction of a pion-nucleus potential through which the pions propagate between their collisions and refers to the real part of the pion optical potential. The imaginary part is included by the nonperturbative description of elementary rescattering and reabsorption processes and is directly medium corrected via the respective densities of nucleons and resonances. Hence, a consistent treatment of the real and imaginary part of the optical potential was achieved.

The pion potential was extracted from the dispersion relation given in the Δ -hole model thereby mixing the pionlike and the Δ -hole-like branches in order to avoid some unphysical features of the model. This, however, leads to a strong softening of the medium effects. Thus, we also applied a phenomenological dispersion relation with a pronounced medium dependence.

Studying the influence of such effects, the different approaches have been subjected to a comparison to the experiment for two contrary observables, i.e., spectra and in-plane flow. Thereby one has to keep in mind that pions at the freeze-out are remnants of a complex collision history, i.e., of multiple creation and reabsorption processes. The analysis of the DIOGENE flow data implies a preferential absorption of pions by the spectator matter known as the shadowing effect which may even lead to an anticorrelation of the collective pion and nucleon in-plane flow. However, a strong attractive pion potential leads to a bending of the pions by the nucleons and thus was found to favor a correlation of the respective flow. The magnitude of this effect is directly proportional to the strength of the potential. Since the pions get bound by the participant matter (slow pions) as well as by the spectator matter (fast pions), this process is complex, i.e., an enhancement of the low p_t range as well as of the high p_t range was observed in transverse momentum spectra.

A comparison to experiments, i.e., the TAPS spectra and to the DIOGENE flow data, seems to rule out a too attractive optical potential. Hence, the pions created in intermediate energy heavy ion collisions are far from the limit of pion condensation. The weak effective Δ -hole potential has nearly no influence on pionic observables as well as the dependence on the nuclear equation of state was found to be rather weak. However, in particular, the spectra of high-energetic pions react sensitively on the dynamics and the present results would favor a pion potential whose attraction is weak at low energies, but becomes more pronounced with increasing energy. In our opinion a furthergoing analysis of high-energetic subthreshold spectra as, e.g., measured in Ref. [8] may help to clarify the question if conventional approaches as, e.g., energy accumulating multiscattering processes or the creation of higher resonances are sufficient to explain such data. The present results indicate that the inclusion of in-medium corrections to the real part of the pion optical potential is of essential importance for a correct description of pion dynamics. In addition, the analysis of the pion in-plane flow also in symmetric systems as, e.g., recently measured by the FOPI collaboration, will help one to learn something about the pion dispersion relation from heavy ion collisions.

- [1] V. Metag, *Prog. Part. Nucl. Phys.* **30**, 75 (1993).
- [2] W. Ehehalt, W. Cassing, A. Engel, U. Mosel, and G. Wolf, *Phys. Rev. C* **47**, R2467 (1993).
- [3] J. W. Harris *et al.*, *Phys. Rev. Lett.* **58B**, 463 (1987).
- [4] D. Brill *et al.*, *Phys. Rev. Lett.* **71**, 336 (1993).
- [5] L. Venema *et al.*, TAPS Collaboration, *Phys. Rev. Lett.* **71**, 835 (1993).
- [6] O. Schwalb *et al.*, TAPS Collaboration, *Phys. Lett. B* **321**, 20 (1994).
- [7] C. Müntz *et al.*, KaoS Collaboration, *Z. Phys. A* **352**, 175 (1995).
- [8] A. Gillitzer *et al.*, *Z. Phys. A* **354**, 3 (1996).
- [9] S. A. Bass, C. Hartnack, H. Stöcker, and W. Greiner, *Phys. Rev. C* **51**, 3343 (1994).
- [10] Bao-An Li, W. Bauer, and G. F. Bertsch, *Phys. Rev. C* **44**, 2095 (1991).
- [11] J. Gosset *et al.*, DIOGENE Collaboration, *Phys. Rev. Lett.* **62**, 1251 (1989).
- [12] C. Hartnack, H. Stöcker, and W. Greiner, in “Proceedings on the International Workshop on Gross Properties of Nuclei and Nuclear Excitation,” XVI, Hirschegg, Kleinwalsertal, Austria, 1988, edited by H. Feldmeier (unpublished).
- [13] J. Zipprich, C. Fuchs, E. Lehmann, L. Sehn, S. W. Huang, and Amand Faessler, *J. Phys. G* (to be published).
- [14] K. Stricker, H. McManus, and J. A. Carr, *Phys. Rev. C* **19**, 929 (1979).
- [15] T. Ericson and W. Weise, *Pions and Nuclei* (Clarendon, Oxford, 1988).
- [16] B. Friedmann, V. R. Pandharipande, and Q. N. Usmani, *Nucl. Phys.* **A372**, 483 (1981).
- [17] C. Gale and J. Kapusta, *Phys. Rev. C* **35**, 2107 (1987).
- [18] J. Aichelin, *Phys. Rep.* **202**, 233 (1991).
- [19] D. T. Khoa, N. Ohtsuka, M. A. Matin, A. Faessler, S. W. Huang, E. Lehmann, and R. K. Puri, *Nucl. Phys.* **A548**, 102 (1992).
- [20] J. Aichelin and H. Stöcker, *Phys. Lett. B* **176**, 14 (1986).
- [21] G. F. Bertsch and S. Das Gupta, *Phys. Rep.* **160**, 190 (1988).
- [22] S. Huber and J. Aichelin, *Nucl. Phys.* **A573**, 587 (1994).
- [23] P. Danielewicz and G. F. Bertsch, *Nucl. Phys.* **A533**, 712 (1991).
- [24] W. H. Dickhoff, A. Faessler, H. Müther, and S. S. Wu, *Nucl. Phys.* **A405**, 534 (1987).
- [25] W. Ehehalt, W. Cassing, A. Engel, U. Mosel, and Gy. Wolf, *Phys. Lett. B* **298**, 31 (1993).
- [26] L. Xiong, C. M. Ko, and V. Koch, *Phys. Rev. C* **47**, 788 (1993).
- [27] R. Averbeck, private communication for the TAPS Collaboration.
- [28] F. D. Berg *et al.*, *Z. Phys. A* **340**, 297 (1990).
- [29] C. Odyniec *et al.*, LBL Report 24580, 215 (1988).